Formation of vortex dipoles

Y. D. Afanasyev[a)]
Department of Physics and Physical Oceanography, Memorial University of Newfoundland, St. John's, Newfoundland A1B 3X7, Canada

(Received 23 August 2005; accepted 7 February 2006; published online 28 March 2006)

Evolution of a two-dimensional flow induced by a jet ejected from a nozzle of finite size is studied experimentally. Vortex dipole forms at the front of the developing flow while a trailing jet establishes behind the dipole. The dynamics of the flow is discussed on the basis of detailed measurements of vorticity and velocity fields which are obtained using particle image velocimetry. It is found that dipoles do not separate (pinch-off) from the trailing jet for values of the stroke ratio up to 15, which fact can be contrasted with the behavior of vortex rings reported previously by other authors. A characteristic time scale that is defined differently from the formation time of vortex rings can be introduced. This time scale (startup time) indicates the moment when the dipole starts translating after an initial period when it mainly grows absorbing the jet from the nozzle. A simple model that considers the competing effects of expansion and translation is developed to obtain an estimate of the dimensionless startup time. The dynamics of a dipole after the formation is characterized by a reduced flux of vorticity from the jet. The dipole moves forward with constant speed such that a value of the ratio of the speed of propagation of the dipole to the mean velocity of the jet is found to be 0.5. A universality of this ratio is explained in the framework of a model based on conservation of mass and momentum for the moving dipole. *© 2006 American Institute of Physics*. [DOI: 10.1063/1.2182006]

I. INTRODUCTION

Vortex dipoles (pairs) are a very well known feature of (quasi-) two-dimensional (2D) flows. Two-dimensionality of the flow can be due to different factors including geometrical restrictions such as those for flows in thin layers or soap films, background rotation of the system, or density stratification. These flows often occur in a stratified rotating ocean. In an oceanographic context, vortex dipoles are often called mushroom-like currents since they resemble a sliced mushroom. Vortex dipoles are formed in a viscous fluid when a (continuous or impulsive) force is applied locally to some volume of fluid. A useful idealization of a localized force is a point force. If a jet from a nozzle is used to reproduce the action of a force the point force can be obtained in the limit when the size D of the nozzle tends to zero while the injection velocity U_{jet} is increased such that the momentum flux per unit depth proportional to $U_{\mathrm{jet}}^2 D$ remains constant. The volume flux per unit depth $U_{\mathrm{jet}}D$, on the other hand, becomes negligible. This idealization was used to obtain theoretical solutions for starting vortex dipole using the Stokes (Cantwell[1]) or the Oseen (Afanasyev and Korabel[2]) approximation. The same approach was used to interpret the results of laboratory experiments. A review of the experimental and theoretical results as related to 2D flows and flows in a stratified fluid is given in Voropayev and Afanasyev.[3] The finite size of the source of the jet, however, can be important especially when the flow in the vicinity of the source is considered. The volume flux from the source is an additional control parameter of the problem in this case. Dimensional analysis[2] shows that the flow is governed by two dimensionless parameters $\Pi_1 = Jt^{1/2}/\nu^{3/2}$ and $\Pi_2 = Ja/\nu^2$, which include kinematic viscosity ν, time t, the momentum flux J (per unit depth and unit density), and the size of the region where the momentum flux (force) is applied, a (equivalent to D in present notation). The parameter Π_1 is effectively the Reynolds number of the flow while the parameter Π_2 represents the effect of the finite size of the source. The analysis[2] of both laboratory experiments and numerical simulations where the forcing was applied in the area of finite size demonstrated that the dynamics of the dipoles does depend on the parameter Π_2. Furthermore, recent laboratory experiments (Afanasyev and Korabel[4]) where a localized force was placed in a uniform stream to simulate a motion of a bluff body demonstrated that the finite size of the forcing area was a necessary condition for the occurrence of regular vortex streets similar to Kármán-Bénard vortex streets behind a cylinder.

It is important to review here some results on vortex rings since the approach to this problem was somewhat different although the flow itself is in fact a three-dimensional (3D) (axisymmetric) analog of a vortex dipole. An experimental arrangement where fluid is ejected from a round nozzle by a piston is most often used to generate vortex rings. This method of generation is natural considering numerous practical applications in nature and industry where the dynamics of vortex rings is important. These applications include in particular the propulsion of some aquatic animals (Dabiri *et al.*[5]). The method of generation that includes a cylindrical pipe with a piston implies that the size of the source is important. Note that an alternative example where a jet from a very small nozzle was used was demonstrated in

[a)]Electronic mail: yakov@physics.mun.ca

experiments by Voropayev and Filippov.[6] In the experiments of Gharib *et al.*[7] the nozzle-piston geometry was used to consider large ratios of the stroke of the piston to the nozzle diameter (long jets) in contrast to previous experiments of other authors where only short ratios were investigated. Two distinct states of the flow were observed in their experiments. While the flows generated by small stroke ratios were in the form of single vortex rings, the flows for large stroke ratios showed a leading vortex ring with an unstable trailing jet posterior to the ring. The transition between the regimes occurred at a mean stroke ratio of approximately 4. The separation of the leading vortex ring from the trailing jet was referred to as vortex ring pinch-off. The circulation of the vortex ring attained a maximum value at this point and did not grow further. Gharib *et al.*[7] and Mohseni and Gharib[8] showed that experimental results are consistent with the Kelvin-Benjamin variational principle, which states that a steady vortex ring must have maximum energy for a given impulse and circulation. Linden and Turner[9] offered a theoretical model where the properties of the ejected fluid were matched to the corresponding properties of the family of vortex rings of different core size and found the same limiting values of the stroke ratio. Existence of a formation time scale for vortex rings was further confirmed in numerical simulations by Rosenfeld *et al.*[10] The idea of a universal formation time that proved to be valid for the formation of the vortex rings was then extended to 2D flows by Jeon and Gharib.[11] These authors considered the initial development and subsequent shedding of vorticity behind a cylinder, which was brought to motion from the state of rest. They found a similarity between the cylinder flow and the formation process of the vortex rings in the fact that a characteristic time exists for bluff-body flows. They attributed this formation time to the onset of asymmetry in the wake behind the cylinder.

Taking into account a general importance of studying the effect of the finite size of the source for the dynamics of starting vortex dipoles as well as looking from another perspective, which includes the investigation of formation and possible separation similar to that discovered for the vortex rings, it is interesting and important to investigate the 2D flow in a geometry similar to that used for vortex rings. Herein we present the results of a new series of experiments where the starting dipoles were generated in a relatively thin layer of fluid by a jet ejected from a channel with a piston. We will also present the results of the theoretical analysis that allows us to obtain the translational velocity of the dipoles during both the initial period of their development as well as for larger times.

II. THEORY

A. Potential flow generated by forces or sources distributed along a line

Consider the initial development of a 2D flow induced by a jet ejected from a nozzle in the form of a line between the points $y=-D/2$ and $y=-D/2$ on the y axis (Fig. 1). For the sake of simplicity, let us choose a "top hat" distribution of velocity in the jet such that $u=U_{\mathrm{jet}}$ on the line and $u=0$

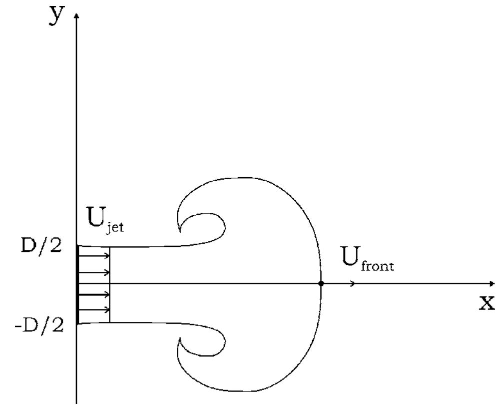

FIG. 1. Sketch of the flow induced by injection of fluid from the nozzle.

otherwise. Here u is the x component of velocity. The jet delivers a volume $Q=U_{\mathrm{jet}}D$ and kinematic momentum $J=U_{\mathrm{jet}}^2D$ per unit time that are the main control parameters of the flow. These parameters are therefore fluxes of mass and momentum normalized by the density of the fluid. The jet generates vorticity when it enters initially quiescent fluid. This vorticity is in the form of two starting vortices of opposite sign located at both flanks of the jet. These vortices together with the jet between them constitute a starting vortex dipole. The vorticity is transported in the fluid with a finite rate by advection and viscous diffusion and remain concentrated in the dipole. Consider a (Lagrangian) fluid particle located at the x axis just in front of the propagating vortex dipole where the flow is approximately irrotational. To obtain the distance traveled by the particle (or equivalently the distance traveled by the front of the starting dipole) we have to integrate the potential flow field induced by the distribution of velocity and pressure at the nozzle. However, it is not a straightforward procedure because, strictly speaking, the distributions of velocity and pressure at the nozzle that constitute the boundary condition for this problem are not known. The top hat velocity profile in the jet can be considered only in the asymptotic steady-state limit. Both pressure and velocity at the boundary may evolve with time in the developing flow. Consider two cases that correspond to potential flows generated either by a distribution of force or the distribution of sources at the boundary. Although neither of these flows provide "ideal" boundary conditions (as we will see later), they do satisfy integral boundary conditions such that these flows are governed by the total force J or the total mass flux Q. These cases are therefore important and can be considered in a sense of providing intermediate asymptotics of the general flow.

The solution of a problem for the flow generated by a point force[1] can provide us with a Green's function for the present problem of a force distributed along a line. The solution is obtained by solving a linearized equation of motion with a singularity at the origin:

$$\frac{\partial \mathbf{u}}{\partial t} = -\frac{1}{\rho}\nabla p + \mathbf{A}\,\delta(\mathbf{x}), \tag{1}$$

where $\mathbf{u}$ is the velocity vector, p is pressure, $\mathbf{x}=(x,y)$ is the position vector, and $\delta(\mathbf{x})$ is the Dirac delta function. The vector **A** represents the force of magnitude $JH(t)$ applied in the positive direction along the x axis. Here $H(t)$ is the Heaviside step function. The solution of (1) together with the equation of continuity gives a pressure field in the form

$$\frac{1}{\rho}p = \frac{Jx}{2\pi(x^2+y^2)}. \tag{2}$$

The velocity potential can be found simply by integration of pressure (2) with respect to time:

$$\varphi = -\frac{1}{\rho}pt. \tag{3}$$

The velocity field is given by

$$\mathbf{u} = -Jt \cdot \frac{1}{2\pi}\nabla\left(\frac{x}{x^2+y^2}\right). \tag{4}$$

The potential for the flow induced by the force distributed along the line can then be found by integration in the Green's function sense:

$$\begin{aligned}\varphi &= -\frac{Jtx}{2\pi D}\int_{-D/2}^{D/2}\frac{dy'}{x^2+(y-y')^2}\\ &= \frac{Jt}{2\pi D}\left[\arctan\left(\frac{y-D/2}{x}\right) - \arctan\left(\frac{y+D/2}{x}\right)\right].\end{aligned} \tag{5}$$

The distribution of pressure at the boundary ($x=0$) for this flow is in the form of a top hat with a value

$$\frac{1}{\rho}p = \frac{J}{D} = U_{\text{jet}}^2$$

along the line representing the nozzle. The velocity field can be easily obtained by finding a gradient of (5). It can be easily shown that the velocity field has singularities at the points $y=\pm D/2$. To describe the motion of a particle along the x axis we have to solve an ordinary differential equation:

$$\frac{dx}{dt} = u(x,y=0,t) = \frac{Jt}{2\pi}\left(\frac{1}{x^2+(D/2)^2}\right). \tag{6}$$

This allows us to obtain the time as a function of distance L_f traveled by the front of the dipole:

$$\begin{aligned}t &= \sqrt{\frac{4\pi}{J}\left[\frac{L_f^3}{3} + \left(\frac{D}{2}\right)^2 L_f\right]}\\ &= \frac{D}{U_{\text{jet}}}\sqrt{4\pi\left[\frac{1}{3}\left(\frac{L_f}{D}\right)^3 + \frac{1}{4}\frac{L_f}{D}\right]}.\end{aligned} \tag{7}$$

Consider now the second case of interest when the flow is induced by sources distributed along a line rather than by a force. Integration along the line similar to that performed in (5) but with the Green's function in the form

$$\varphi = \frac{Q}{2\pi}\log\sqrt{x^2+y^2}, \tag{8}$$

allows us to obtain the velocity potential. The expression for the potential is not given here because it is quite lengthy. The x component of velocity can be obtained in a more compact form as follows:

$$u = -\frac{Q}{2\pi D}\left[\arctan\left(\frac{y-D/2}{x}\right) - \arctan\left(\frac{y+D/2}{x}\right)\right]. \tag{9}$$

The potential and the velocity field for this case are stationary in contrast to the previous case when these fields increase linearly with time. The boundary conditions at the nozzle are also different. For the latter case the distribution of x component of velocity (9) is of top hat form at $x=0$, but the pressure is singular along the line representing the nozzle. The distance traveled by the front of the flow can again be easily obtained in the form of the following relation:

$$t = \frac{\pi}{U_{\text{jet}}}\int_0^{L_f}\frac{dx}{\arctan[D/(2x)]}. \tag{10}$$

B. Steady-state regime

Finally, let us consider larger times of the evolution of the flow when the dipole has moved far away from the nozzle and the trailing jet is established behind the dipole. A simple physical model of the flow can be developed based on the integral relations expressing some conservation laws (e.g., Voropayev *et al.*[12]). A vortex dipole can again be related to a finite volume of fluid within which the motion is essentially vortical and outside of which the motion is approximately irrotational. This volume moves in the fluid and its size increases. The balance of mass and momentum for the fluid volume V are

$$\frac{dV}{dt} = (U_{\text{jet}} - U_f)D, \tag{11}$$

$$(1+k)\frac{dVU_f}{dt} = U_{\text{jet}}(U_{\text{jet}} - U_f)D, \tag{12}$$

where k is the added mass coefficient. (Precisely speaking, V is the area of the dipole in our 2D model.) Here it is assumed that the dipole moves slower than the trailing jet ($U_f < U_{\text{jet}}$) such that the jet constantly delivers mass and momentum into the dipole. The additional influx into the dipole due to entrainment of ambient fluid is assumed to be small compared to influx from the jet and is neglected in (11). Note that the entrained fluid can constitute a significant part of the volume of a single vortex ring (without trailing jet) according to measurements by Dabiri and Gharib.[13] The relative unimportance of entrainment in our case is due to either the different (planar) geometry of our problem or to different dynamics because of the effect of the trailing jet is subject to verification by comparison of the results of the model with the experiments. Making the further assumption that the velocity of the dipole U_f does not depend on time (which will be confirmed later in our experiments), a simple relation between the velocity of the dipole and the velocity of the jet can be obtained:

$$U_f = \frac{1}{1+k}U_{\text{jet}}. \tag{13}$$

Since the potential flow induced by a moving dipole is equivalent to that of the moving cylinder, the same value of

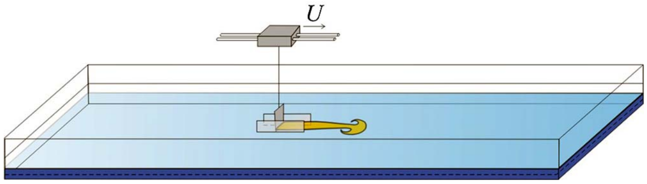

FIG. 2. (Color online) Sketch of the experimental setup.

the added mass coefficient $k=1$ can be employed here to yield $U_f=U_{\mathrm{jet}}/2$. Note that the analogy between the flow around a dipole and the cylinder flow is quite straightforward and follows in particular from the Chaplygin-Lamb solution (e.g., Meleshko and van Hejst[14]) for the inviscid dipole.

III. EXPERIMENTAL TECHNIQUE

The laboratory experiments reported herein were carried out in a long rectangular tank of dimensions 120×30 cm where a channel-piston arrangement was installed. The schematics of the setup is shown in Fig. 2. The tank was filled with two layers of water of different density. The upper layer was fresh water while the lower layer was saline water of concentration 250 g/l. Most of the experiments were performed in water where the depth of each layer was 1.1 cm, although lower values of 0.4 and 0.8 cm were also tested in different experiments. No significant dependence on the depth of the layers was observed. Two layers were used to minimize the vertical component of velocity, providing the two-dimensionality of the flow (e.g., Paret *et al.*[15]). The two-layer system was similar to that used in our previous experiments with 2D turbulence (Wells and Afanasyev[16]). That system was shown to work well in achieving the purpose of two-dimensionality of the flow. In a thin layer system bottom friction is an important factor that prevents the flow from being purely 2D. Bottom friction as well as friction due to ordinary viscosity causes the total energy of the flow to decay (e.g., Danilov *et al.*[17]). It is important therefore to maintain a rate of energy decrease due to bottom friction that is somewhat less than that due to ordinary viscosity. This was demonstrated to be the case in Wells and Afanasyev,[16] where the depth of each layer was 0.5 cm. We assume that this is also true for the present experiments where the depth of the layers was greater then that used previously.

Another important phenomenon associated with flows in a thin stratified layer is generation of internal waves. The parameters of the flow under study should then be chosen such that the effect of internal waves is negligible. To estimate the characteristics of the internal waves in the system consider the parameters of the stratification in the tank. The tank was initially filled very carefully to avoid any mixing. The filling process typically took 5–10 min. Assuming that diffusion starts immediately we can estimate the evolution of the vertical density distribution in the system. Solving the equation of diffusion with no-flux boundary conditions at the surface and at the bottom and step-like initial distribution of concentration, one obtains by separation of variables

$$c(z,t)=\sum_{n=1,n-odd}\frac{2}{\pi n}\sin\left(\frac{2\pi n}{H}z\right)\exp\left(-\kappa\frac{4n^2\pi^2}{H^2}t\right).$$

Here $H=2.2$ cm is the total depth of the fluid and $\kappa=1.1$ 10^{-5} cm/s is the coefficient of diffusion of salt in water. Vertical profiles of the concentration c can then be calculated easily for different times. Immediately after the filling stops the initial step-like distribution is smoothed by diffusion. Although the diffusion is very fast initially when the gradient of concentration is very high, it slows down with time such that even after 1 h, the density difference still remains large. Typically, one series of experiments was finished within a 1 h period after what the tank was refilled. The value of buoyancy frequency at the interface varies from $N=10$ s^{-1} immediately after the filling to $N=6$ s^{-1} after a 1 h period. These values of buoyancy frequency correspond to the values of the period $T=0.6$–1 s. The characteristic time (6–45 s) of the piston translation was much larger in our experiments such that we can reasonably expect that the flows are hydraulically well adjusted. Indeed, further measurements of the velocity field of the flow show no significant unsteady effects that might be associated with internal waves. Note that the energy loss associated with the emission of the internal waves by unsteady quasi-2D dipoles is small (of the order of a few percent) even when the stratification is much weaker and the flow is closer to a resonance. It was shown to be the case for colliding vortex dipoles (Afanasyev[18]). In our present experiments internal waves were only observed when the piston was stopped suddenly after translation in the channel at the end of each run. The waves can then be noticed by the modulation of the interface. Although there was no evidence of significant wave emission at the start or during the motion of the piston certain precautions were made to eliminate the effects of possible reflection of the waves from the side walls of the tank. For this purpose the sloping beaches made from sponge were installed at the sides of the tank.

The flow in the tank was induced by a jet ejected from a channel located in the middle of the tank. A jet was induced by a piston translating along the channel in the horizontal direction. The piston extended through the depth of the fluid in the container such that the distance between the lower edge of the piston and the bottom was less than 0.1 cm. The piston was towed by a traversing system driven by a computer controlled stepping motor. The piston was started impulsively with a very short ($\sim$0.1 s) acceleration period and then moved with constant velocity. The piston velocity was varied in the range $U_p=0.4$–4 cm/s for different experiments. Channels of width 1.2 and 1.8 cm with the walls made of thin Plexiglas were used in our experiments. A few series of experiments were also performed in a different geometry. A channel of larger width $D_{\mathrm{ch}}=2.4$ cm with a slit at the exit was used for this purpose. The width of the slit was $D=0.7$, 1.2, or 1.7 cm. While for the experiments with the channel the mean velocity of the jet U_{jet} at the exit was equal to the velocity of the piston, for the experiments with the slit, the value of U_{jet} was obtained from the volumetric relation $U_{\mathrm{jet}}=U_pD_{\mathrm{ch}}/D$. Direct measurements of velocity at the exit of the slit confirmed the accuracy of this relation.

The flow was recorded using a digital video camera with

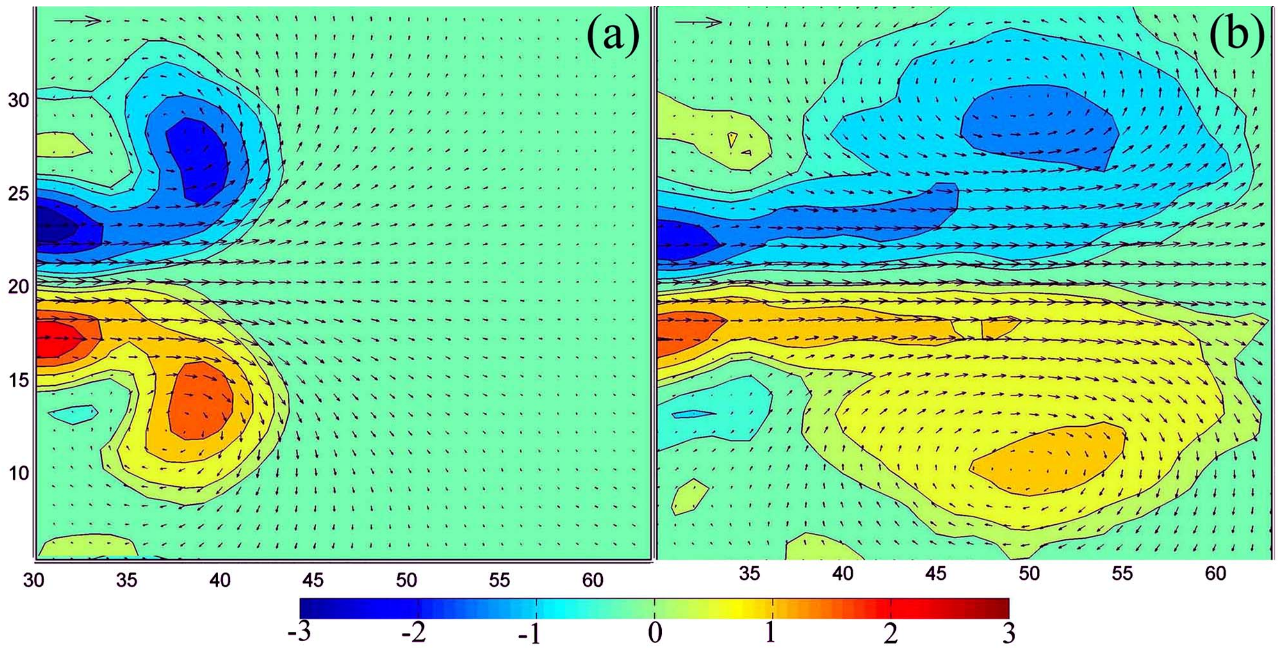

FIG. 3. (Color online) Velocity (arrows) and vorticity (contours) fields: $t=5.3$ (a) and 14.2 s (b). Parameters of the experiment: $D=1.8$ cm (channel), $U_{\text{jet}}=0.75$ cm/s. Arrow in the right upper corner of each panel represents the velocity scale 2 cm/s. Color bar shows the vorticity scale in s^{-1}. Unit step in x and y direction is 0.18 cm.

an array resolution of 1288×1032 placed above the container. The horizontal velocity field in the flow was measured using a particle image velocimetry (PIV) technique. A description of the particular methods used in our PIV code is given by Fincham and Spedding[19] and Pawlak and Armi.[20] Filtration and interpolation of velocity data during the post-processing stage of the PIV analysis were performed using a variational technique (Afanasyev and Demirov[21]). The seeding particles were polyamid spheres of mean diameter 50 μm and density 1.03 g/cm^3. The density of the particles corresponds to the density of water with a salt concentration of approximately 37 g/l. A suspension of particles in water of neutral density was introduced into the interface between the layers. The particles were made visible by illuminating the interface between the layers with a sheet of light from a 1 W argon ion laser. Image sequences with a frame rate of 12.5 fps were recorded directly into the memory buffers of a computer. Further processing of the images that had a pixel resolution of approximately 90 pixels/cm was performed using the PIV code to obtain velocity fields of dimensions 44×77 vectors.

IV. EXPERIMENTAL RESULTS AND INTERPRETATION

In order to identify different regimes of the flow a number of experiments were performed where the main control parameters, namely the velocity of the jet U_{jet}, the width of the slit (or the width of the channel) D, and the length of translation of the piston along the channel L have been varied. A typical evolution of vorticity in the flow is shown in Fig. 3. Part of the flow within the channel near the exit is also visible at the right-hand side of the pictures. The images show that when the jet emerges from the channel it splits and wraps around two starting vortices [Fig. 3(a)]. Later the vortices join to form a dipole that starts propagating forward [Fig. 3(b)].

Although our initial expectations were to observe the separation (pinch-off) of the dipole from the trailing jet such as that reported for vortex rings (see, e.g., Figs. 13 and 18 in Ai *et al.*[22]), these expectations were not realized. The pinch-off was not observed in any of our experiments. The image in Fig. 4 demonstrates the dipole with a trailing jet visualized by particles. The photograph was taken with a large exposure such that the streaks show the regions of high velocity. The boundary of the jet is clearly visible in the picture and the dipole forms a continuous flow with the trailing jet. Only after the motion of the piston was stopped, the dipole entrained the remainder of the trailing jet and then propagated on its own. However, the issue on whether the separation occurs can only be resolved on the basis of measurements of

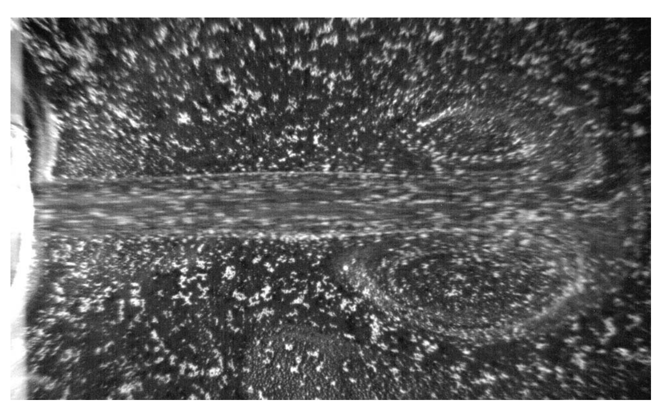

FIG. 4. Vortex dipole with a trailing jet visualized by particles. Parameters of the experiment: $U_{\text{jet}}=2.7$ cm/s, $D=0.7$ cm, $L/D=51$, slit geometry.

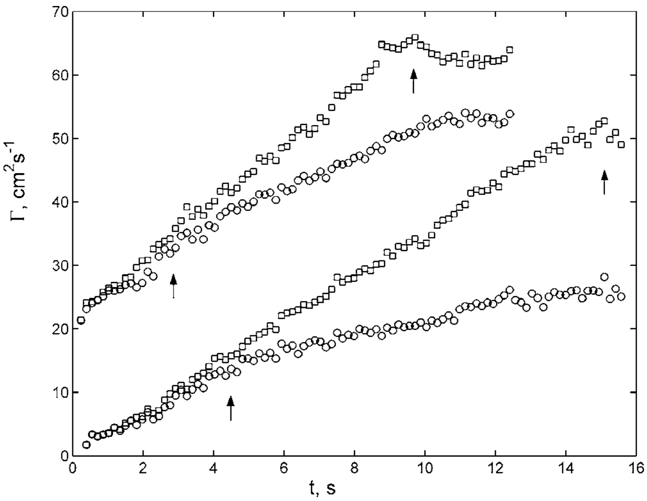

FIG. 5. Area integrated absolute value of vorticity for the entire flow (squares) and for the dipole (circles) for two different experiments. Arrows indicate the formation times of the dipoles and the times when the piston was stopped in each experiment. Parameters of the experiments: $U_{\mathrm{jet}}=1.6$ cm/s, $D=1.2$ cm, and $U_{\mathrm{jet}}=2.7$ cm/s, $D=1.7$ cm, slit geometry. The graph for the second experiment is shifted up by 20 to avoid the overcrowding.

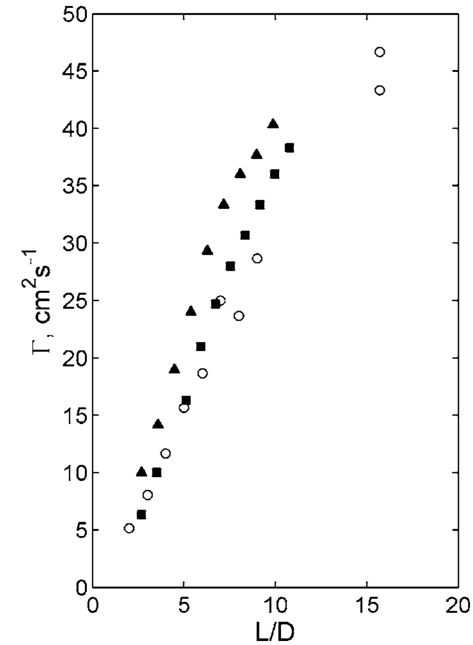

FIG. 6. Maximum value of the area integrated vorticity in the dipole for different values of the maximum piston displacement. Parameters of the experiments: $U_{\mathrm{jet}}=2.7$ cm/s, $D=1.2$ cm, slit (circles), and channel geometry (squares); $U_{\mathrm{jet}}=1.9$ cm/s, $D=1.8$ cm, channel geometry (triangles).

the total vorticity in the dipole rather than on a visual assessment. These measurements were performed in all of our experiments using the following method. A rectangular region that includes the entire dipole (determined by the extent of the contour line of 5% of maximal vorticity) was drawn manually on vorticity maps obtained by the PIV for each time step. The area integrals of the absolute value of vorticity were calculated for the selected region as well as for the entire flow field. These quantities have units of circulation and, if calculated only for a vortex of either positive or negative sense in the dipole, do represent the circulation in the vortex. Typical results of these measurements showing the evolution of the total vorticity in the dipole and in the entire flow are demonstrated in Fig. 5 for two experiments with different values of the jet velocity U_{jet}. Both plots show that the vorticity for the entire flow increases in an approximately linear fashion until the motion of the piston stops ($t=9$ and 15 s). The vorticity of the dipole initially follows the total vorticity (in fact, the dipole cannot be separated from the jet at this stage). The dipole is not translating appreciably during this initial period but rather growing in size, absorbing all of the fluid ejected from the channel. At some moment of time ($t_s=3$ and 4.5 s) the flow exhibits a change of regime when the growth of vorticity in the dipole becomes slower than that for the entire flow. We will call this a startup time of the dipole to distinguish it from the formation time (as introduced in Ref. 7 for vortex rings), which is rather associated with the pinch-off of a leading vortex. After the startup time the dipole starts translating while being continuously attached to the jet. The dipole is fed by the fluid from the trailing jet such that the total vorticity of the dipole continues to grow linearly with time although with a somewhat lower rate than that of the entire flow. The rest of the vorticity supplied by the flow from the channel is accumulated in the growing trailing jet. Thus two distinct regimes of the flow can be identified before and after the transition at the characteristic startup time. Note that after the piston was stopped the total circulation of the leading vortex must approach that of the entire flow. Indeed, if the dipole is not detached from the trailing jet it eventually entrains all of the circulation ejected by the vortex generator. One might argue that the trends in the plots in Fig. 5 (upper curves) do not suggest this behavior. However, a dip in both plots that is observed after the piston is stopped is rather due to a perturbation by an interfacial wave that is generated when the piston is stopped suddenly at the entrance of the channel (this effect is discussed in the previous section). After the perturbation, the total circulation returns to a plateau while the circulation of the dipole continues to grow until it reaches the value of the total circulation. Since the perturbation was quite strong, the data collected after the perturbation were considered to be unreliable and was discarded in most of our experiments.

To further confirm the observation that the dipole is continuously attached to the jet for the entire range of piston strokes available in our experimental setup, we conducted a few series of experiments where the piston performed limited excursions along the channel. Here we followed the method used by Gharib *et al.*[7] in their experiments with vortex rings. The maximum distance traveled by the piston normalized by the diameter of the channel, L/D, is equivalent to the dimensionless time of piston translation. Note that in the experiments with the slit, the distance L was obtained from the volumetric relation $L=L_pD_{\mathrm{ch}}/D$, where L_p is the maximum distance traveled by the piston in channel of width D_{ch}. This distance represents the translation the piston would perform in the channel of the width equal to the width of the slit to push the same volume of fluid. Figure 6 depicts the maximum values of total vorticity in the dipole for different val-

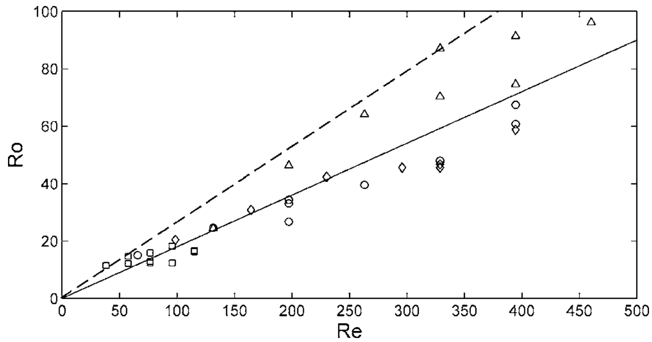

FIG. 7. The Roshko number vs the Reynolds number for different experiments. Parameters of the experiments: $D=0.7$ cm (slit), $U_{\text{jet}}=0.9$–2.8 cm/s (squares); $D=1.2$ cm (slit), $U_{\text{jet}}=0.5$–3.3 cm/s (circles); $D=1.2$ cm (channel), $U_{\text{jet}}=0.5$–3.3 cm/s (diamonds); $D=1.7$ cm (slit), $U_{\text{jet}}=0.7$–2.7 cm/s (triangles).

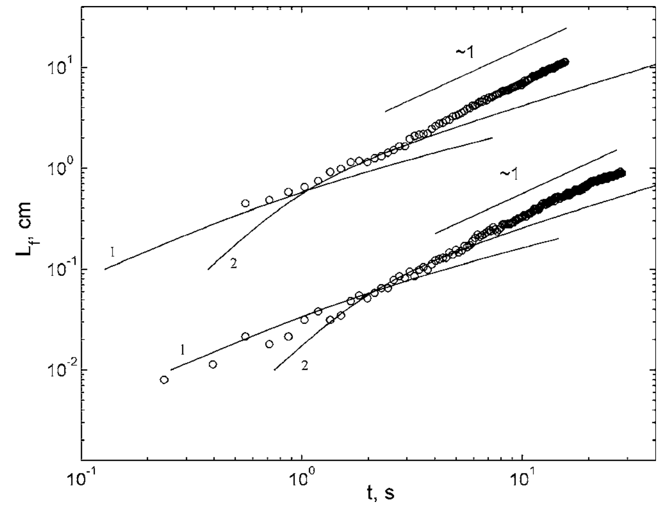

FIG. 8. Distance from the nozzle to the front of the dipole for two experiments: $D=1.2$ cm, $U_{\text{jet}}=0.8$ cm/s, channel; $D=1.2$ cm, $U_{\text{jet}}=1.6$ cm/s, slit. The data for the channel experiment are shifted down by a decade to avoid the overcrowding. Labels 1 and 2 indicate the lines representing relations (10) and (7), respectively.

ues of L/D. While for vortex rings the circulation reaches a plateau at $L/D\approx 4$ (e.g., Fig. 6 in Gharib *et al.*[7]), for vortex dipoles it continues to grow at least until $L/D=15$.

Values of the startup time t_s were measured in all of our experiments that were performed for different values of the dimensional control parameters U_{jet} and D for both the channel and slit geometries. In order to better understand the behavior of t_s, it is useful to first perform a simple dimensional analysis. The startup time t_s depends on a set of 3D quantities including U_{jet} and D and the kinematic viscosity. In fact, this set of parameters is exactly the same as that for the flow around a circular cylinder. The width of the channel is then equivalent to the diameter of the cylinder while the velocity of the jet corresponds to the velocity of the stream. The dimensional analysis then gives

$$\frac{D^2}{t_s\nu}=\Phi\left(\frac{U_{\text{jet}}D}{\nu}\right), \tag{14}$$

where Φ is an unknown function of one dimensionless argument, the Reynolds number Re. To follow the analogy with cylinder flow we will call the dimensionless parameter in the left-hand side of (14) the Roshko number Ro. Note that the dimensional analysis can be done also in terms of other dimensionless parameters, namely the Reynolds number and the Strouhal number defined as $\text{St}=U_{\text{jet}}/(t_sD)$. The Strouhal number is the reciprocal of the dimensionless startup number. Figure 7 demonstrates the plot of Ro versus Re, where linear fit gives $\text{Ro}=0.18\text{Re}+0.02$. Hypothesizing that a similarity exists between the starting dipole flow and the flow around the cylinder, the data in Fig. 7 can be compared with a well-known linear dependence between the Roshko and the Reynolds numbers for the cylinder flow, $\text{Ro}=0.212(\text{Re}-21.2)$ (Roshko[23]).

It is interesting and important to investigate the details of the physical process that leads to the formation of the dipole and its subsequent translation at the front of the trailing jet. Some insight into the evolution of a starting dipole can be provided by measurements of the propagation of the front of the flow. The distance L_f measured from the exit of the channel towards the front of the dipole is shown in Fig. 8 as a function of time for two experiments. These experiments were for slit and channel geometries with the same value of D. The results, however, are typical for all of our experiments. The results demonstrate that during the initial period for times smaller than the startup time $(t<t_s)$, the dipole propagates relatively slow. Observations show that the vortices of the dipole grow during this stage without significant translation forward. The solid lines in Fig. 8 show the theoretical relations (7) and (10) that describe the motion due to potential flow generated by the injection from the nozzle. Comparison of theory with the experimental data shows that the model where the expansion of fluid is due to sources distributed along a line describes well an initial development of the flow immediately after the startup. Another model where the forces distributed along the line are considered provides reasonable intermediate asymptotics for the flow evolution during the initial period. After this initial period the vorticity generated at the nozzle becomes dynamically important and the flow can no longer be described by potential flow theories. At later times $(t>t_s)$, L_f varies approximately linearly with time such that the dipole moves with constant speed. The values of the speed of the front U_f were measured in the experiments with different values of U_{jet} and are shown in Fig. 9. The data collapse well on the straight

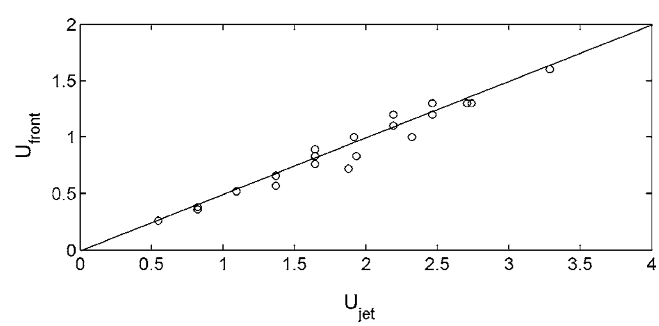

FIG. 9. Speed of the propagation of the front of the dipole for the experiments with different values of the injection velocity U_{jet}.

line. A linear fit gives the dependence $U_f = cU_{\text{jet}}$, where the value of the slope is $c = 0.50 \pm 0.02$. This value is in good agreement with the theoretical prediction (13).

On the basis of these observations a simple model can be proposed to elucidate (at least in the qualitative manner) the dynamics of the startup of the flow. Consider an idealized setup where a nozzle is represented by a source of mass and momentum. Suppose that a dipolar vortex has just occurred within a circular patch of fluid of diameter D. The source supplies fluid with a rate $U_{\text{jet}}D$ (per unit depth) such that the patch expands. The area V of the patch increases linearly with time:

$$V = \pi D^2/4 + U_{\text{jet}} D t, \tag{15}$$

such that the radius R of the patch grows as $R = (V/\pi)^{1/2}$. The source also supplies (kinematic) momentum $U_{\text{jet}}^2 D$ per unit depth. As a result, the patch starts translating. The speed U of the patch can be estimated from momentum balance (12), where the right-hand side is simply the momentum supplied by the source and V is substituted using (15). Integration of the resulting equation gives

$$U = U_{\text{jet}} \frac{\tau}{(\tau + \pi/4)(1+k)}, \tag{16}$$

where $\tau = tU_{\text{jet}}/D$ is the dimensionless time. Thus the leading vortex dipole translates as a whole with velocity U while expanding uniformly according to (15). When the rear end of the dipole passes the origin, a trailing jet must form. This corresponds to the startup time as defined above. Subtracting the distance that a point at the rear end of the dipole would cover due to expansion and translation and equating the result to zero, one obtains a simple transcendental equation. The numerical solution of this equation gives the dimensionless startup time $\tau_s = 3.8$. This result is shown by a dashed line in Fig. 7. The model clearly underestimates the startup time. However, it is hardly possible to expect a better performance from this relatively crude model that does not in particular take into account the effects of friction or the presence of solid walls within the flow.

V. DISCUSSION

In summary, it can be concluded that the results of the laboratory experiments reported in this article provide evidence that a time scale that characterizes the dynamics of starting vortex dipoles can be introduced. This time scale is named a startup time. It indicates the moment when the dipole starts translating after an initial period of time when it mainly grows absorbing the jet from the nozzle. A simple model that considers the competing effects of expansion and translation allows us to obtain an estimate of the dimensionless startup time. Note that a similar model was earlier developed for 3D flows where dipoles were generated by injecting fluid from a round nozzle in a stratified fluid.[24] Due to the different geometry of these problems the dynamics is different. In a stratified case a regime when a dipole is developing within an intrusion was observed. In that case the expansion prevails over the translation. This is due to the fact that both the speed of expansion and the speed of translation are proportional to $t^{-1/2}$. It is then the ratio of the coefficients of proportionality that defines the regime of the flow. For the 2D flows considered here, translation always prevails with time due to the different time dependence of the speed of translation. As a consequence, a characteristic startup time can be introduced. Note that the simple model developed here to describe the startup dynamics does not take into account viscous effects that can reduce the translation speed of the dipole, especially for low values of the Reynolds number. This effect might cause the occurrence of the regime where the dipole does not propagate but just expands such that the startup time is infinite. Whether a limiting value of the Reynolds number below which the dipoles do not form the trailing jet exists is certainly an interesting question that deserves further attention.

When the dipole translates, the trailing jet establishes behind the dipole. As a result, the total vorticity flux supplied by the jet issuing form the nozzle is shared between the dipole and the trailing jet such that the growth of total vorticity in the dipole becomes slower than that in the entire flow. Our experiments demonstrate that vortex dipoles do not separate from the trailing jet for the values of the stroke ratio up to $L/D = 15$. This observation can be contrasted with the results for the vortex rings (Gharib *et al.*[7]) where a complete separation (pinch-off) was observed at a dimensionless formation number of approximately 4. Although the pinch-off of the leading vortex dipole from the trailing jet was not observed in any of our experiments, the existence of finite "pinch-off" time (formation number[7]) is certainly a possibility for larger values of the stroke ratio L/D. After the present paper had been completed, results of numerical simulations (Winckelmans[25]) were brought to our attention. The 2D flow from a channel was simulated by the viscous vortex particle method. The sequence of vorticity maps of the flow demonstrates that, at dimensionless time $\tau = U_{\text{jet}}t/D = 25$, the leading vortex dipole is clearly pinched off from the trailing jet while at $\tau = 20$ it is yet completely attached. While further numerical simulations and perhaps newly designed laboratory experiments are required to obtain more details of the pinch-off of the vortex dipoles, some predictions can be made using theoretical arguments similar to those used in Refs. 8 and 9 for vortex rings. A plug model of the flow from the channel gives the volume V_p per unit depth, the circulation (in the half-plane) and the energy per unit depth E_p in the following form:

$$V_p = DL, \tag{17}$$

$$\Gamma_p = U_{\text{jet}} L/2, \tag{18}$$

$$E_p = U_{\text{jet}}^2 V_p/2 = U_{jet}^2 DL/2. \tag{19}$$

These properties can be matched to those of the vortex dipole resulting from the injection of the plug fluid. To parameterize the properties of dipoles, a theoretical model similar to that by Norbury[26] for vortex rings is required. Pierrehumbert[27] constructed a one-parameter family of steady translating vortex dipoles with uniform vorticity distributed within some closed area. The properties of the dipoles, including the normalized kinetic energy E_n, were com-

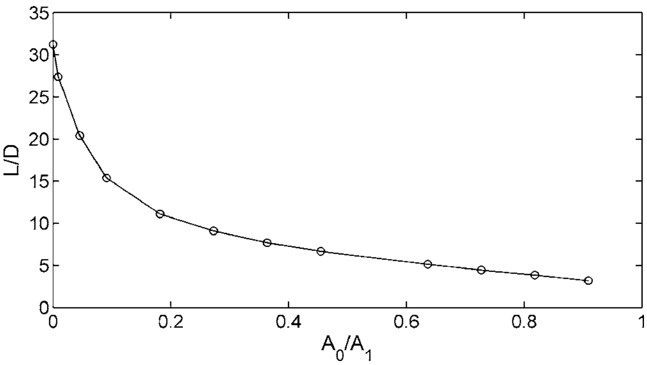

FIG. 10. The aspect ratio L/D of the plug generated by the piston/channel arrangement plotted against the parameter A_0/A_1 for the corresponding vortex dipole, calculated using (20) and the data tabulated in Table 1 of Pierrehumbert (Ref. 27).

puted and tabulated. Assuming that circulation and energy are conserved in the formation process of the dipole, we use (18) and (19) to obtain

$$\frac{L}{D} = \frac{2}{E_n}. \tag{20}$$

This ratio is plotted in Fig. 10 as a function of parameter A_0/A_1 that parameterizes the dipole family.[27] Here A_0 is the minimum distance of the boundary of the vortex patch from the symmetry axis and A_1 is the maximum distance. The ratio A_0/A_1 therefore defines how concentrated the vorticity is in the dipole. The limiting cases are $A_0/A_1 \to 1$ when the dipole consists of almost point vortices and $A_0/A_1 \to 0$ when the vortices touch the symmetry axis. Since all of the dipoles observed in our experiments belonged to a category with the axis touching vorticity, it is reasonable to expect high values of the stroke ratio, perhaps in the range between 15 and 32. Given such high values of the stroke ratio, we must also take into account that the actual time when the pinch-off is observed can be significantly higher than the formation time because it takes additional time for the dipole to absorb all of the fluid from the trailing jet. Thus the experimental observation of the pinch-off seems to require a large size apparatus. Perhaps numerical simulations provide a better opportunity here, especially because higher values of the Reynolds number can be achieved and consequently vortex dipoles with thinner cores can be produced for which the formation number is significantly lower.

ACKNOWLEDGEMENTS

The research reported in this paper has been supported by the Natural Sciences and Engineering Research Council of Canada under Grants No. 300805-04 and No. 227192-04. The author is grateful to J. Wells for help in conducting the experiments.

[1]B. J. Cantwell, "Viscous starting jets," J. Fluid Mech. **173**, 159 (1986).
[2]Y. D. Afanasyev and V. N. Korabel, "Starting vortex dipoles in a viscous fluid: Asymptotic theory, numerical simulations and laboratory experiments," Phys. Fluids **16**, 3850 (2004).
[3]S. I. Voropayev and Y. D. Afanasyev, *Vortex Structures in a Stratified Fluid* (Chapman and Hall, London, 1994).
[4]Y. D. Afanasyev and V. N. Korabel, "Wakes and vortex streets generated by translating force and force doublet: Laboratory experiments," J. Fluid Mech. **553**, 119 (2006).
[5]J. O. Dabiri, S. P. Colin, J. H. Costello, and M. Gharib, "Flow patterns generated by oblate medusan swimmers: *In situ* observation and analysis," J. Exp. Biol. **208**, 1257 (2005).
[6]S. I. Voropayev and I. A. Filippov, "Development of a horizontal jet in homogeneous and stratified fluids: laboratory," Izv. Akad. Nauk SSSR, Fiz. Atmos. Okeana **21**, 964 (1985).
[7]M. Gharib, E. Rambod, and K. Shariff, "A universal time scale for vortex ring formation," J. Fluid Mech. **360**, 121 (1998).
[8]K. Mohseni and M. Gharib, "A model for universal time scale of vortex ring formation," Phys. Fluids **10**, 2436 (1998).
[9]P. F. Linden and J. S. Turner, "The formation of 'optimal' vortex rings, and the efficiency of propulsion devices," J. Fluid Mech. **427**, 61 (2001).
[10]M. Rosenfeld, E. Rambod, and M. Gharib, "Circulation and formation number of laminar vortex rings," J. Fluid Mech. **376**, 297 (1998).
[11]D. Jeon and M. Gharib, "On the relationship between the vortex formation process and cylinder wake vortex patterns," J. Fluid Mech. **519**, 161 (2004).
[12]S. I. Voropayev, Y. D. Afanasyev, and I. A. Filippov, "Horizontal jets and vortex dipoles in a stratified fluid," J. Fluid Mech. **227**, 543 (1991).
[13]J. O. Dabiri and M. Gharib, "Fluid entrainment by isolated vortex rings," J. Fluid Mech. **511**, 311 (2004).
[14]V. V. Meleshko and G. J. F. van Heijst, "On Chaplygin's investigations of two-dimensional vortex structures in an inviscid fluid," J. Fluid Mech. **272**, 157 (1994).
[15]J. Paret, D. Marteau, O. Paireau, and P. Tabeling, "Are flows electromagnetically forced in thin stratified layers two dimensional," Phys. Fluids **9**, 3102 (1997).
[16]J. Wells and Y. D. Afanasyev, "Decaying quasi-two-dimensional turbulence in a rectangular container: laboratory experiments," Geophys. Astrophys. Fluid Dyn. **98**, 1 (2003).
[17]S. Danilov, F. V. Dolzhanskii, V. A. Dovzhenko, and V. A. Krymov, "Experiments on free decay of quasi-two-dimensional turbulent flows," Phys. Rev. E **65**, 036316 (2002).
[18]Y. D. Afanasyev, "Spontaneous emission of gravity waves by interacting vortex dipoles in a stratified fluid: laboratory experiments," Geophys. Astrophys. Fluid Dyn. **97**, 79 (2003).
[19]A. Fincham and G. Spedding, "Low cost, high resolution DPIV for measurement of turbulent fluid flow," Exp. Fluids **23**, 449 (1997).
[20]G. Pawlak and L. Armi, "Vortex dynamics in a spatially accelerating shear layer," J. Fluid Mech. **376**, 1 (1998).
[21]Y. D. Afanasyev and E. K. Demirov, "Variational filtration and interpolation technique for PIV employing fluid dynamical constraints," Exp. Fluids **39**, 828 (2005).
[22]J. J. Ai, A. W.-K. Law, and L. P. Chua, "Vortex dynamics in starting square water jets," Phys. Fluids **17**, 014106 (2005).
[23]A. Roshko, "On the development of turbulent wakes from vortex streets," Ph.D. thesis, California Institute of Technology (1952).
[24]Y. D. Afanasyev, S. I. Voropayev, and A. A. Kudin, "Vortex dipole inside a homogeneous intrusion in a density stratified fluid," Izv., Acad. Sci., USSR, Atmos. Oceanic Phys. **28**, 193 (1992).
[25]G. S. Winckelmans (private communication).
[26]J. Norbury, "A family of steady vortex rings," J. Fluid Mech. **57**, 417 (1973).
[27]R. T. Pierrehumbert, "A family of steady, translating vortex pairs with distributed vorticity," J. Fluid Mech. **99**, 129 (1980).